

## Lifetime of the Bose Gas with Resonant Interactions

B. S. Rem,<sup>1</sup> A. T. Grier,<sup>1</sup> I. Ferrier-Barbut,<sup>1</sup> U. Eismann,<sup>1</sup> T. Langen,<sup>2</sup> N. Navon,<sup>1</sup> L. Khaykovich,<sup>1,3</sup> F. Werner,<sup>1</sup> D. S. Petrov,<sup>4,5</sup> F. Chevy,<sup>1</sup> and C. Salomon<sup>1</sup>

<sup>1</sup>Laboratoire Kastler-Brossel, École Normale Supérieure, CNRS and UPMC, 24 rue Lhomond, 75005 Paris, France

<sup>2</sup>Vienna Center for Quantum Science and Technology, Atominstytut, TU Wien, Stadionallee 2, 1020 Wien, Austria

<sup>3</sup>Department of Physics, Bar-Ilan University, Ramat-Gan, 52900 Israel

<sup>4</sup>Université Paris-Sud, CNRS, LPTMS, UMR8626, Orsay F-91405, France

<sup>5</sup>Russian Research Center Kurchatov Institute, Kurchatov Square, 123182 Moscow, Russia

(Received 20 December 2012; published 16 April 2013)

We study the lifetime of a Bose gas at and around unitarity using a Feshbach resonance in lithium 7. At unitarity, we measure the temperature dependence of the three-body decay coefficient  $L_3$ . Our data follow a  $L_3 = \lambda_3/T^2$  law with  $\lambda_3 = 2.5(3)_{\text{stat}}(6)_{\text{syst}} \times 10^{-20} (\mu\text{K})^2 \text{cm}^6 \text{s}^{-1}$  and are in good agreement with our analytical result based on zero-range theory. Varying the scattering length  $a$  at fixed temperature, we investigate the crossover between the finite-temperature unitary region and the previously studied regime where  $|a|$  is smaller than the thermal wavelength. We find that  $L_3$  is continuous across the resonance, and over the whole  $a < 0$  range our data quantitatively agree with our calculation.

DOI: [10.1103/PhysRevLett.110.163202](https://doi.org/10.1103/PhysRevLett.110.163202)

PACS numbers: 34.50.Lf, 03.65.Nk, 31.15.xj, 67.85.-d

Recent advances in manipulating cold atomic vapors have enabled the study of Fermi gases at the unitary limit where the scattering length  $a$  describing two-body interactions becomes infinite. It has been demonstrated both experimentally and theoretically that in this limit the system is characterized by a scale invariance leading to remarkably simple scaling laws [1]. In contrast, most experimental results on Bose-Einstein condensates were obtained in the weakly interacting regime. Recent experimental results on bosons near Feshbach resonances have revived the interest in strongly interacting bosons [2]: the development of experimental tools has enabled a precise test of the Lee-Huang-Yang corrections [3,4], and several theoretical papers have studied the hypothetical unitary Bose gas at zero [5–8] or finite [9] temperature. The strongly interacting Bose gas is one of the most fundamental quantum many-body systems, yet many open questions remain. Examples include the prediction of weakly bound Efimovian droplets [10,11], the existence of both atomic and molecular superfluids [12], and the creation of strongly correlated phases through three-body losses [13].

Experimental investigation of ultracold bosons near unitarity has been hampered by the fast increase of the three-body recombination rate close to a Feshbach resonance [14,15]. In this case, the number of trapped atoms  $N(t)$  follows the usual three-body law

$$\dot{N} = -L_3 \langle n^2 \rangle N, \quad (1)$$

where  $\langle n^2 \rangle = \int d^3r n^3(\mathbf{r})/N$  is the mean square density and  $L_3$  is the three-body loss rate constant. In the zero-temperature limit  $L_3$  increases as  $\hbar a^4/m$  [16] multiplied by a dimensionless log-periodic function of  $a$  revealing Efimov physics [17–26]. At finite temperature,  $L_3$  saturates when  $a$  becomes comparable to the thermal wavelength

$\lambda_{\text{th}} = h/\sqrt{2\pi m k_B T}$ , and  $L_3 \sim \hbar a^4/m \sim \hbar^5/m^3 (k_B T)^2$  [9,27,28]. This saturation suggests that a non-quantum-degenerate Bose gas near a Feshbach resonance will maintain thermal quasiequilibrium [9]. Indeed, in this regime,  $|a| \geq \lambda_{\text{th}}$  and  $n\lambda_{\text{th}}^3 \ll 1$ . Thus, the elastic collision rate  $\gamma_2 \propto \hbar \lambda_{\text{th}} n/m$  is much higher than the three-body loss rate  $\gamma_3 = L_3 n^2 \propto \hbar \lambda_{\text{th}}^4 n^2/m$ . Experimental and numerical evidence for a saturation of  $L_3$  was reported in Refs. [3,22,27]. A theoretical upper bound compatible with this scaling was derived in Ref. [29] assuming that only the lowest three-body hyperspherical harmonic contributes, an assumption which breaks down when  $|a|$  exceeds  $\lambda_{\text{th}}$ .

In this Letter, we measure the temperature dependence of the unitary three-body recombination rate and find agreement with a  $L_3 \propto 1/T^2$  scaling law. In a second set of measurements performed at constant temperature, we study  $L_3$  versus  $a$ . We show how this function smoothly connects to the zero-temperature calculations when  $|a| \ll \lambda_{\text{th}}$ . These observations are explained by a general theoretical result for  $L_3(a, T)$ , exact in the zero-range approximation, that we derive in the second part. Our theory allows for a complete analytic description of the unitary case and, in particular, predicts (weak) log-periodic oscillations of the quantity  $L_3 T^2$ . Our findings quantify the ratio of good-to-bad collisions in the system and provide solid ground for future studies of strongly interacting Bose gases. Furthermore, on the  $a < 0$  side, experiments have so far detected a single Efimov trimer [3,23–25,30]. Our analysis predicts that a second Efimov trimer of very large size should be detectable in  ${}^7\text{Li}$  at temperatures on the order of a few microkelvins.

Our experimental setup was presented in Ref. [4]. After magneto-optical trapping and evaporation in an Ioffe magnetic trap down to  $\approx 30 \mu\text{K}$ ,  $\approx 2 \times 10^6$   ${}^7\text{Li}$  atoms are transferred into a hybrid magnetic and dipole trap in

the state  $|1, 1\rangle$ . The transverse confinement is obtained by a single laser beam of waist  $43(1) \mu\text{m}$  and wavelength  $1073 \text{ nm}$ , while the longitudinal trapping is enhanced by a magnetic field curvature. The resulting potential has a cylindrical symmetry around the propagation axis of the laser and is characterized by trapping frequencies  $0.87 < \omega_\rho/2\pi < 3.07 \text{ kHz}$  and  $18 < \omega_z/2\pi < 49 \text{ Hz}$ . Further cooling is achieved by applying a homogeneous magnetic field  $B \simeq 718 \text{ G}$  for which the scattering length is  $\simeq 200a_0$ , and decreasing the depth of the trapping potential down to a variable value  $U'$  allowing us to vary the final temperature of the cloud. Afterwards, the dipole trap is recompressed to a value  $U > U'$ , to prevent significant atom loss due to the enhanced evaporation rate; see below. At each  $T$  we choose  $U$  so as to maintain the temperature constant during the three-body loss rate measurement. Finally, the magnetic field is ramped in  $100\text{--}500 \text{ ms}$  to  $B_0 \simeq 737.8(3) \text{ G}$ , where the scattering length  $a$  diverges [4]. We then measure the total atom number  $N$  remaining after a variable waiting time  $t$  and the corresponding  $T$ , using *in situ* imaging of the thermal gas.

Our data are limited to the range of temperature  $1 \leq T \leq 10 \mu\text{K}$ . For  $T \geq 1 \mu\text{K}$ , the rate  $\gamma_3 = -\dot{N}/N$  remains small with respect to other characteristic rates in our cloud (elastic scattering rate, trapping frequencies), which guarantees that a thermal quasiequilibrium is maintained. We check that for these parameters the *in situ* integrated density profile is indeed Gaussian, and we use it to extract the temperature of the cloud, found to be in agreement with that of time of flight. The peak phase-space density varies within  $0.07 \times 10^{-2} < n_0 \lambda_{\text{th}}^3 < 1.1 \times 10^{-2}$ . A typical time dependence of  $N$  and  $T$  is shown in Fig. 1. The time dependence of the atom number is fitted using the usual three-body recombination law Eq. (1) [31]. For a nondegenerate gas of temperature  $T$ , the density profile is Gaussian,

and we have  $\langle n^2 \rangle = N^2 A(T) = N^2 (m \bar{\omega}^2 / 2\pi \sqrt{3} k_B T)^3$ , with  $\bar{\omega} = (\omega_\rho^2 \omega_z)^{1/3}$  being the mean trapping frequency. We then have

$$\dot{N} = -L_3(T) A(T) N^3. \quad (2)$$

Assuming constant temperature, integrating Eq. (2) gives

$$N(t) = \frac{N(0)}{\sqrt{1 + 2A(T)L_3(T)N^2(0)t}}, \quad (3)$$

which we use as a fitting function to analyze  $N(t)$ , and extract  $L_3(T)$  as shown in Fig. 1.

Because of their  $n^3/T^2$  dependence, three-body losses preferentially remove atoms of low kinetic energy and those located at the center of the trap where the density is the highest and potential energy is the smallest. As a result, three-body loss events heat up the cloud [16]. We ensure constant temperature by operating with a typical trap depth  $U \simeq \eta k_B T$  with  $6 \leq \eta \leq 8$ , for which the residual evaporation then balances recombination heating; see Fig. 1(b). This ensures that  $L_3$  is time independent, but, as a drawback, evaporation contributes to losses. To quantify the relative importance of evaporative and three-body losses, we first note that an atom expelled by evaporation removes on average an energy  $\simeq (\eta + \kappa) k_B T$ , where, taking  $\kappa$  from Ref. [32], we follow Ref. [33]. Typically, we have  $\kappa \simeq 0.68$  for  $\eta = 6$  and  $\kappa \simeq 0.78$  for  $\eta = 8$  [34]. In comparison, each three-body event leaves on average an excess heat of  $\delta k_B T$  per particle. Extending the derivation of Ref. [16] to the case of an energy dependent three-body loss rate  $\propto E^{-2}$ , we obtain  $\delta = 5/3$  [34]. The energy balance required to keep the temperature constant thus implies that the evaporation rate is  $\simeq \delta/(\eta + \kappa - 3)$  times smaller than the three-body loss rate. Neglecting this effect would induce a systematic overestimation of  $L_3$  of about 50% for  $\eta = 6$  and 30% for  $\eta = 8$ . Therefore, we apply this systematic correction to our data.

The temperature dependence of  $L_3$  obtained from our measurements at unitarity is shown in Fig. 2. It is well fit by the scaling law  $L_3(T) = \lambda_3/T^2$ , with  $\lambda_3 = 2.5(3)_{\text{stat}} \times 10^{-20} (\mu\text{K})^2 \text{cm}^6 \text{s}^{-1}$  as the best-fit value. In order to discuss the systematic uncertainty of this measurement, we note that the quantity  $L_3 T^2$  scales in all experimental parameters identically to the thermodynamic quantity  $(\mu^2/P)^2$  of a zero-temperature Bose-Einstein condensate with chemical potential  $\mu$  and pressure  $P$  [34]. We use this relation to calibrate our experimental parameters [4] and obtain a systematic uncertainty on  $\lambda_3$  of  $\leq 25\%$  resulting in  $\lambda_3 = 2.5(3)_{\text{stat}}(6)_{\text{syst}} \times 10^{-20} (\mu\text{K})^2 \text{cm}^6 \text{s}^{-1}$ .

We now study the  $a$  dependence of  $L_3$  on both sides of the resonance by employing the same experimental procedure as in the unitary case. We tune the scattering length while keeping the temperature within 10% of  $5.9 \mu\text{K}$ ; see Fig. 3. The excess heat  $\delta$  entering in the correction now depends on the value of  $ka$ . The correction is applied to all data points (filled circles) except in the range  $1500a_0 < a < 5000a_0$  (open circles), where the assumptions of our

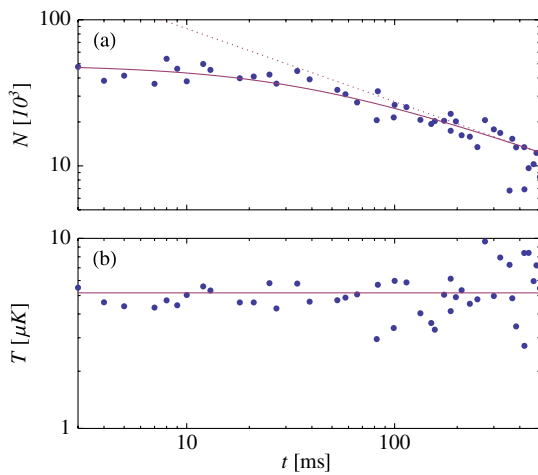


FIG. 1 (color online). Time dependence of the atom number (a) and temperature (b) for  $U = \eta k_B T$ , with  $T = 5.2(4) \mu\text{K}$ ,  $\eta = 7.4$ , and (uncorrected)  $L_3 = 1.2(2)_{\text{stat}} \times 10^{-21} \text{cm}^6 \text{s}^{-1}$ . The dotted line shows the long time  $t^{-1/2}$  dependence of the number of atoms.

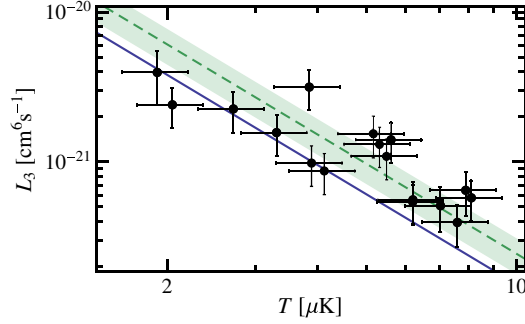


FIG. 2 (color online). Temperature dependence of the three-body loss rate  $L_3$ . Filled circles, experimental data; green dashed line, best fit to the data  $L_3(T) = \lambda_3/T^2$  with  $\lambda_3 = 2.5(3)_{\text{stat}}(6)_{\text{syst}} \times 10^{-20} (\mu\text{K})^2 \text{cm}^6 \text{s}^{-1}$ ; the shaded green band shows the  $1\sigma$  quadrature sum of uncertainties. Solid line, prediction from Eq. (5),  $\lambda_3 = 1.52 \times 10^{-20} (\mu\text{K})^2 \text{cm}^6 \text{s}^{-1}$  with  $\eta_* = 0.21$  from Refs. [30,39].

model are not applicable [34]. In the limit  $|a| \gg \lambda_{\text{th}}$ , we observe that  $L_3(a)$  saturates to the same value on both sides of the resonance. In the opposite limit  $|a| \ll \lambda_{\text{th}}$ , our data connect to the zero-temperature behavior [20] studied experimentally in Refs. [22–26]. On the  $a < 0$  side, the dashed line is the zero-temperature prediction for  $L_3$  from Ref. [20]. We clearly see that finite temperature reduces the three-body loss rate. On the  $a > 0$  side, temperature effects become negligible for  $a < 2000a_0$ , as testified by our measurements performed on a low-temperature Bose-Einstein condensate (green squares), which agree with the total recombination rate to shallow and deep dimers calculated at  $T = 0$  in Ref. [20] (dashed line). The data around unitarity and on the  $a < 0$  side are seen to be in excellent agreement with our theory Eq. (4) described below.

In order to understand the dependence  $L_3(a, T)$  theoretically, we employ the  $S$ -matrix formalism developed in Refs. [20,35,36]. According to the method, at hyperradii  $R \gg |a|$  one defines three-atom scattering channels ( $i = 3, 4, \dots$ ) for which the wave function factorizes into a normalized hyperangular part  $\Phi_i(\hat{R})$  and a linear superposition of the incoming,  $R^{-5/2}e^{-ikR}$ , and outgoing,  $R^{-5/2}e^{ikR}$ , hyperradial waves. The channel  $i = 2$  is defined for  $a > 0$  and describes the motion of an atom relative to a shallow dimer. The recombination or relaxation to deep molecular states (with a size of order the van der Waals range  $R_e$ ) requires inclusion of other atom-dimer channels. In the zero-range approximation, valid when  $R_e \ll R_m \equiv \min(1/k, |a|)$ , the overall effect of these channels and all short-range physics in general can be taken into account by introducing a single Efimov channel ( $i = 1$ ) defined for  $R_e \ll R \ll R_m$ : the wave function at these distances is a linear superposition of the incoming,  $\Phi_1(\hat{R})R^{-2+is_0}$ , and outgoing,  $\Phi_1(\hat{R})R^{-2-is_0}$ , Efimov radial waves. Here  $s_0 \approx 1.00624$ . The notion “incoming” or “outgoing” is defined with respect to the long-distance region  $R_m \lesssim R \lesssim |a|$ , so that, for example, the incoming Efimov wave actually propagates towards larger  $R$  whereas incoming waves in all other channels propagate

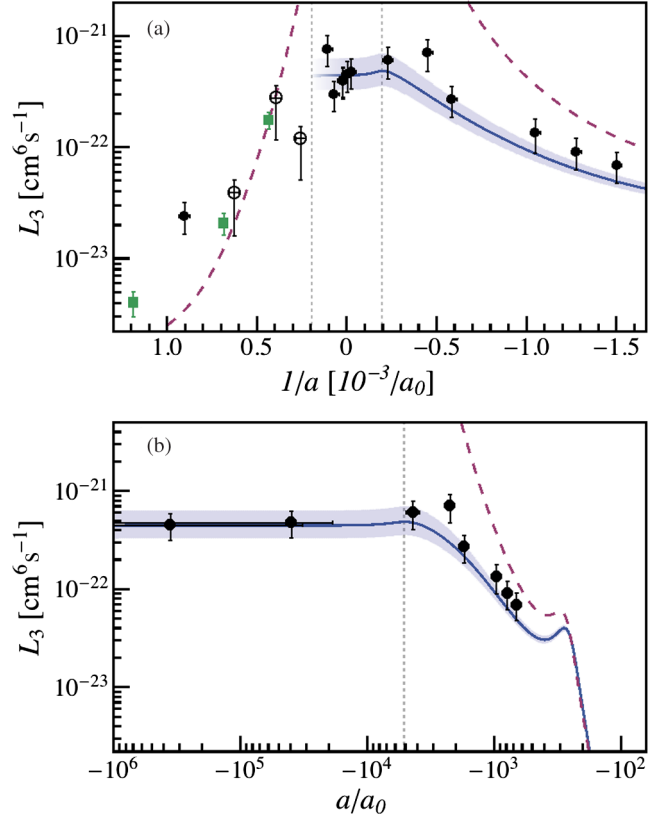


FIG. 3 (color online). (a)  ${}^7\text{Li}$  scattering-length dependence of the three-body rate constant  $L_3(a)$  for constant  $T = 5.9(6) \mu\text{K}$  (filled and open circles). For small positive  $a$ ,  $L_3(a)$  for a low-temperature condensate is also shown (green squares). The solid blue line corresponds to our theoretical prediction Eq. (4) for  $T = 5.9 \mu\text{K}$ . The blue range is the same theory for  $5.3$  to  $6.5 \mu\text{K}$ . The dashed lines show the zero-temperature prediction for  $L_3(a)$  [20] fitted to the measurements in Refs. [30,39] with the parameters  $\eta_* = 0.21$  and  $R_0 = 270a_0$ . The vertical dotted lines correspond to  $|a|/\lambda_{\text{th}} = 1$ . The open circles in the range  $1500a_0 < a < 5000a_0$  are not corrected for residual evaporation as our model is not applicable. (b) Logarithmic plot of the  $a < 0$  side, displaying the two Efimov loss resonances.

towards smaller hyperradii. The matrix  $s_{ij}$  relates the incoming amplitude in the  $i$ th channel with the outgoing one in the  $j$ th channel and describes the reflection, transmission, and mixing of channels in the long-distance region. This matrix is unitary and independent of the short-range physics. The short-range effects are taken into account by fixing the relative phase and amplitude of the incoming and outgoing Efimov waves  $R^2\Psi \propto (R/R_0)^{is_0} - e^{2\eta_*}(R/R_0)^{-is_0}$ , where  $R_0$  is the three-body parameter and the short-range inelastic processes are parametrized by  $\eta_* > 0$ , which implies that the number of triples going towards the region of  $R \sim R_e$  is by the factor  $e^{4\eta_*}$  larger than the number of triples leaving this region [37]. Braaten *et al.* [36] have shown that for a given incoming channel  $i \geq 2$  the probability of recombination to deeply bound states is  $P_i = (1 - e^{-4\eta_*})|s_{i1}|^2 / [1 + (kR_0)^{-2is_0} e^{-2\eta_*} s_{11}]^2$  [38]. For  $a < 0$ , by using the fact that  $s_{11}$  is unitary ( $\sum_{i=1}^{\infty} |s_{i1}|^2 = 1$ ) and averaging over the

Boltzmann distribution, we then obtain the total loss rate constant

$$L_3 = \frac{72\sqrt{3}\pi^2\hbar(1 - e^{-4\eta_*})}{mk_{\text{th}}^6} \times \int_0^\infty \frac{(1 - |s_{11}|^2)e^{-k^2/k_{\text{th}}^2}kdk}{|1 + (kR_0)^{-2is_0}e^{-2\eta_*s_{11}}|^2}, \quad (4)$$

where  $k_{\text{th}} = \sqrt{mk_B T}/\hbar$ .

Note that in deriving Eq. (4) we closely followed [36] where the scattering length was assumed to be finite. However, we easily generalize this derivation to the case  $a = \infty$ , in which the channels become decoupled at distances  $R \gg 1/k$  and the long-distance region can now be defined by  $R \sim 1/k$ . A less trivial result of our analysis is that for any  $ka$  there exists a unitary transformation of the matrix  $s_{ij}$  which leaves the element  $s_{11}$  invariant, but all channels with  $i > 3$  become decoupled from the Efimov channel [34]. This transformation constructs a new large- $R$  channel characterized by a certain hyperangular wave function  $\tilde{\Phi}_3(\hat{R})$ . For negative or infinite  $a$  this is the only channel that can “talk” to the lossy short-distance Efimov channel via a unitary  $2 \times 2$  matrix. Therefore, the three-body loss rate cannot exceed the so-called maximum value  $L_3^{\text{max}} = 36\sqrt{3}\pi^2\hbar^5(k_B T)^{-2}/m^3$  reached in the case when the outgoing flux in this newly constructed channel vanishes. Previous derivations of  $L_3^{\text{max}}$  [29] essentially implied that  $\tilde{\Phi}_3(\hat{R})$  is the lowest *noninteracting* hyperspherical harmonics. This approximation can be made only for  $k|a| \ll 1$ . In general,  $\tilde{\Phi}_3(\hat{R})$  is *not* an eigenstate of the angular momentum operator. In particular, at unitarity  $\tilde{\Phi}_3(\hat{R}) = \Phi_1(\hat{R})$  [34].

The function  $s_{11}(ka)$  is calculated in Ref. [34]. At unitarity it equals  $s_{11}(\infty) = -e^{-\pi s_0} e^{2i[s_0 \ln 2 + \arg \Gamma(1 + is_0)]}$ , and from Eq. (4) one sees that  $L_3 T^2$  should be a log-periodic function of  $T$ . However, due to the numerically small value of  $|s_{11}| \approx 0.04$ , in the case of three identical bosons the oscillations are very small and  $L_3$  is well approximated by setting  $s_{11} = 0$ :

$$L_3 \approx \frac{\hbar^5}{m^3} 36\sqrt{3}\pi^2 \frac{1 - e^{-4\eta_*}}{(k_B T)^2}. \quad (5)$$

This explains the  $L_3 \propto T^{-2}$  experimental observation seen in Fig. 2 at unitarity. Taking  $\eta_* = 0.21$ , which is the average of two measurements made for our  $^7\text{Li}$  Feshbach resonance in Refs. [30,39], we get  $L_3 = \lambda_3/T^2$  with  $\lambda_3 = 1.52 \times 10^{-20} (\mu\text{K})^2 \text{cm}^6 \text{s}^{-1}$ . This is 40% below the experimentally determined value without any adjustable parameter and the agreement between theory and experiment is  $1.4\sigma$ .

We should point out that Eq. (4) can be easily generalized to the case of other three-body systems with smaller  $s_0$ . Then, the terms neglected in Eq. (5) can become important. They also become important in our system of three identical bosons when departing from resonance in the direction of  $a < 0$ . Then  $|s_{11}(ka)|$  monotonically increases as a function of  $1/k|a|$  reaching 1 in the limit

$ka \rightarrow 0^-$ , the argument of  $s_{11}$  also being a monotonic function of  $1/k|a|$  [34]. The solid dark gray (blue) line in Fig. 3 is the result obtained from Eq. (4) using the same  $\eta_*$  as above and  $R_0 = 270a_0$  also taken from Refs. [30,39]. The shaded blue area reflects our experimental range of temperatures. More or less visible maxima of  $L_3$  appear when the denominator in the integrand of Eq. (4) reaches its minimum, i.e., becomes resonant. The approximate condition for this is  $\arg s_{11}(ka) = \pi + 2s_0 \ln kR_0$ , and the features become increasingly more pronounced for larger  $|s_{11}|$  and smaller  $\eta_*$ . Note that from the viewpoint of the visibility of the maxima, decreasing  $|a|$  is equivalent to decreasing  $\sqrt{T}$ . Figure 3(b) shows the pronounced resonance at  $a = a_- \approx -274a_0$  observed in Refs. [30,39]. This resonance is associated with the passage of an Efimov trimer through the three-atom threshold. Another Efimov trimer, larger in size by a factor of  $e^{\pi/s_0} = 22.7$ , is expected to go through the threshold at around  $a \approx -6350a_0$ , leading to another zero energy resonance. As we deduce from Eq. (4) and show in Fig. 3 for  $5.9 \mu\text{K}$ , the thermally averaged remnants of this predicted resonance lead to a maximum of  $L_3$  at  $a \approx -5100a_0$ . As seen in Fig. 3(b), the agreement between theory and experiment is very good over the entire  $a < 0$  range.

Because of the existence of a shallow dimer state, the case  $a > 0$  becomes, in general, a complicated dynamical problem which should take into account the atom-dimer and dimer-dimer relaxation as well as various nonuniversal factors: the finite trap depth, chemical imbalance between trapped shallow dimers and free atoms, and deviations from thermal equilibrium which possibly depend on the preparation sequence. These issues require an extensive discussion beyond the scope of this Letter. The situation obviously simplifies in the case of very small  $a$  when the system is purely atomic and the three-body recombination to deep and shallow molecules leads to an immediate loss of three atoms.

Discussing the opposite limit of large  $a > 0$ , we first note that dimers are well defined when their size  $\sim a$  is smaller than  $n^{-1/3}$ , which we assume in the following (the limit  $na^3 \gg 1$  is equivalent to the case  $a = \infty$ ). In the regime  $a \gg \lambda_{\text{th}}$  we find using the Skorniakov-Ter-Martirosian equation that  $s_{12} \rightarrow 0$  for  $ka \rightarrow \infty$ , which implies that the atom-dimer relaxation rate vanishes; shallow dimers then remain at chemical quasiequilibrium with the decaying atomic ensemble, with a molecular fraction  $\propto n\lambda_{\text{th}}^3 \ll 1$  (for the data of Fig. 3 with  $a > \lambda_{\text{th}}$ , the molecular fraction is 0.6%) [34]. Shallow dimer formation and breakup are then balanced, so that the atomic decay is just given by Eq. (1). The expression of  $L_3$  for  $a > 0$  was obtained in Ref. [36] and reduces to Eq. (4) for  $s_{12} \rightarrow 0$ . We conclude that the loss rate must be continuous across the resonance, in accordance with our experimental data. Therefore, in Fig. 3(a) the result of Eq. (4) is simply continued to positive  $a$  for  $a \gg \lambda_{\text{th}}$ .

In summary, we have systematically studied the dependence of the three-body loss rate on  $T$  and  $a$  in a Bose gas

near unitarity. Equation (5) shows that, at unitarity,  $L_3$  never reaches  $L_3^{\max}$ , and one can hope to produce quantum degeneracy in a unitary Bose gas using atomic species with a particularly small  $\eta_*$ . Note that the loss mechanism in our system drastically differs from a chemical reaction with finite activation energy  $\Delta E$  characterized by the well-known Arrhenius law  $L_3 \propto \exp(-\Delta E/k_B T)$ . In our case, instead of a potential hill there is an effective three-body  $R^{-2}$  attraction leading to  $\Psi(R) \propto (\lambda_{\text{th}}/R)^2$  at distances  $R_e \lesssim R \lesssim \lambda_{\text{th}}$ , where we normalized the three-body wave function  $\Psi$  to unit volume and omitted its log-periodic  $R$  dependence. We clearly see that the probability of finding three atoms in the recombination region is enhanced at small temperatures and scales as  $|\Psi|^2 \propto \lambda_{\text{th}}^4 \propto 1/T^2$ . More subtle is a quantum interference effect in Efimov three-body scattering, which leads to an enhanced decay rate at a negative  $a$ , suggesting the possibility to observe the signature of a second Efimov trimer of large size. Another future direction is to explore the approach to the quantum-degenerate regime and test whether the virial expansion of the unitary Bose gas [40] can be measured by using quasiequilibrium thermodynamics [9].

We acknowledge fruitful discussions with G. Shlyapnikov and F. Ferlaino, and support from Région Île de France (IFRAF), EU (ERC advanced grant Ferlodim), Institut Universitaire de France, and the Russian Foundation for Fundamental Research. T.L. acknowledges support by the Austrian Science Fund (FWF) through the Doctoral Programme CoQuS (W1210).

- 
- [1] *BCS-BEC Crossover and the Unitary Fermi Gas*, Lecture Notes in Physics Vol. 836, edited by W. Zwerger (Springer, Berlin, 2011).
- [2] S. E. Pollack, D. Dries, M. Junker, Y. P. Chen, T. A. Corcovilos, and R. G. Hulet, *Phys. Rev. Lett.* **102**, 090402 (2009).
- [3] R. J. Wild, P. Makotyn, J. M. Pino, E. A. Cornell, and D. S. Jin, *Phys. Rev. Lett.* **108**, 145305 (2012).
- [4] N. Navon, S. Piatecki, K. Günter, B. Rem, T.-C. Nguyen, F. Chevy, W. Krauth, and C. Salomon, *Phys. Rev. Lett.* **107**, 135301 (2011).
- [5] S. Cowell, H. Heiselberg, I. E. Mazets, J. Morales, V. R. Pandharipande, and C. J. Pethick, *Phys. Rev. Lett.* **88**, 210403 (2002).
- [6] J.-L. Song and F. Zhou, *Phys. Rev. Lett.* **103**, 025302 (2009).
- [7] Yu-Li Lee and Yu-Wen Lee, *Phys. Rev. A* **81**, 063613 (2010).
- [8] D. Borzov, M. S. Mashayekhi, S. Zhang, J.-L. Song, and F. Zhou, *Phys. Rev. A* **85**, 023620 (2012).
- [9] W. Li and T.-L. Ho, *Phys. Rev. Lett.* **108**, 195301 (2012).
- [10] J. von Stecher, *J. Phys. B* **43**, 101002 (2010).
- [11] J. von Stecher, *Phys. Rev. Lett.* **107**, 200402 (2011).
- [12] S. Basu and E. J. Mueller, *Phys. Rev. A* **78**, 053603 (2008).
- [13] N. Syassen, D. M. Bauer, M. Lettner, T. Volz, D. Dietze, J. J. Garcia-Ripoll, J. I. Cirac, G. Rempe, and S. Durr, *Science* **320**, 1329 (2008).
- [14] S. Inouye, M. R. Andrews, J. Stenger, H.-J. Miesner, D. M. Stamper-Kurn, and W. Ketterle, *Nature (London)* **392**, 151 (1998).
- [15] J. L. Roberts, N. R. Claussen, S. L. Cornish, and C. E. Wieman, *Phys. Rev. Lett.* **85**, 728 (2000).
- [16] T. Weber, J. Herbig, M. Mark, H.-C. Nägerl, and R. Grimm, *Phys. Rev. Lett.* **91**, 123201 (2003).
- [17] E. Nielsen and J. H. Macek, *Phys. Rev. Lett.* **83**, 1566 (1999).
- [18] B. D. Esry, C. H. Greene, and J. P. Burke, *Phys. Rev. Lett.* **83**, 1751 (1999).
- [19] P. F. Bedaque, E. Braaten, and H.-W. Hammer, *Phys. Rev. Lett.* **85**, 908 (2000).
- [20] E. Braaten and H.-W. Hammer, *Phys. Rep.* **428**, 259 (2006).
- [21] D. S. Petrov, in *Proceedings of the Les Houches Summer Schools, Session 94*, edited by C. Salomon, G. V. Shlyapnikov, and L. F. Cugliandolo (Oxford University Press, Oxford, England, 2013).
- [22] T. Kraemer, M. Mark, P. Waldburger, J. G. Danzl, C. Chin, B. Engeser, A. D. Lange, K. Pilch, A. Jaakkola, H. C. Nägerl, and R. Grimm, *Nature (London)* **440**, 315 (2006).
- [23] M. Zaccanti, B. Deissler, C. D'Errico, M. Fattori, M. Jonas-Lasinio, S. Müller, G. Roati, M. Iguscio, and G. Modugno, *Nat. Phys.* **5**, 586 (2009).
- [24] S. E. Pollack, D. Dries, and R. G. Hulet, *Science* **326**, 1683 (2009).
- [25] N. Gross, Z. Shotan, S. Kokkelmans, and L. Khaykovich, *Phys. Rev. Lett.* **103**, 163202 (2009).
- [26] F. Ferlaino, A. Zenesini, M. Berninger, B. Huang, H. C. Nägerl, and R. Grimm, *Few-Body Syst.* **51**, 113 (2011).
- [27] J. P. D'Incao, H. Suno, and B. D. Esry, *Phys. Rev. Lett.* **93**, 123201 (2004).
- [28] J. P. D'Incao, C. H. Greene, and B. D. Esry, *J. Phys. B* **42**, 044016 (2009).
- [29] N. P. Mehta, S. T. Rittenhouse, J. P. D'Incao, J. von Stecher, and C. H. Greene, *Phys. Rev. Lett.* **103**, 153201 (2009).
- [30] N. Gross, Z. Shotan, S. Kokkelmans, and L. Khaykovich, *Phys. Rev. Lett.* **105**, 103203 (2010).
- [31] We neglect four- and higher-body losses which, dimensionally, are expected to be suppressed by a factor  $n_0 \lambda_{\text{th}}^3$  [29].
- [32] O. Luiten, M. Reynolds, and J. T. M. Walraven, *Phys. Rev. A* **53**, 381 (1996).
- [33] L. Luo, B. Clancy, J. Joseph, J. Kinast, A. Turlapov, and J. E. Thomas, *New J. Phys.* **8**, 213 (2006).
- [34] See Supplemental Material at <http://link.aps.org/supplemental/10.1103/PhysRevLett.110.163202> for more information on the calculation of  $s_{11}$ ; a discussion of  $s_{12}$ , atom-dimer relaxation, and chemical equilibrium in the limit  $a \rightarrow \infty$ ; a construction of the unitary transformation for the matrix  $s_{ij}$ ; an interpretation of Eq. (4) in terms of a Fabry-Perot interferometer; and a discussion of evaporation and experimental uncertainties.
- [35] V. Efimov, *Sov. J. Nucl. Phys.* **29**, 546 (1979).
- [36] E. Braaten, H.-W. Hammer, D. Kang, and L. Platter, *Phys. Rev. A* **78**, 043605 (2008).
- [37] E. Braaten, H.-W. Hammer, and M. Kusunoki, *Phys. Rev. A* **67**, 022505 (2003).
- [38] Our  $s_{11}$  differs by a phase factor from the one defined in Ref. [36]; see Ref. [34].
- [39] N. Gross, Z. Shotan, O. Machtey, S. Kokkelmans, and L. Khaykovich, *C.R. Physique* **12**, 4 (2011).
- [40] Y. Castin and F. Werner, [arXiv:1212.5512v2](https://arxiv.org/abs/1212.5512v2).